

OPTICAL COHERENCE TOMOGRAPHY

PACS numbers: 42.30.Wb; 87.57.N–; 87.64.Cc
DOI: 10.1070/QE2011v041n10ABEH014549

Depth-resolved monitoring of diffusion of hyperosmotic agents in normal and malignant human esophagus tissues using optical coherence tomography *in-vitro*

Qingliang Zhao, Zhouyi Guo, Huajiang Wei, Hongqin Yang, Shusen Xie

Abstract. **Depth-resolved monitoring with differentiation and quantification of glucose diffusion in healthy and abnormal esophagus tissues has been studied *in vitro*. Experiments have been performed using human normal esophagus and esophageal squamous cell carcinoma (ESCC) tissues by the optical coherence tomography (OCT). The images have been continuously acquired for 120 min in the experiments, and the depth-resolved and average permeability coefficients of the 40% glucose solution have been calculated by the OCT amplitude (OCTA) method. We demonstrate the capability of the OCT technique for depth-resolved monitoring, differentiation, and quantifying of glucose diffusion in normal esophagus and ESCC tissues. It is found that the permeability coefficients of the 40% glucose solution are not uniform throughout the normal esophagus and ESCC tissues and increase from $(3.30 \pm 0.09)\times10^{-6}$ and $(1.57 \pm 0.05)\times10^{-5}$ cm s^{-1} at the mucous membrane of normal esophagus and ESCC tissues to $(1.82 \pm 0.04)\times10^{-5}$ and $(3.53 \pm 0.09)\times10^{-5}$ cm s^{-1} at the submucous layer approximately 742 μm away from the epithelial surface of normal esophagus and ESCC tissues, respectively.**

Keywords: *hyperosmotic agents, glucose, permeability, human normal esophagus, esophageal squamous cell carcinoma, optical coherence tomography.*

1. Introduction

Esophageal cancer is one of deadliest cancers worldwide and is the sixth leading cause of death from malignancies [1]. Cancer of the esophagus exists in two main forms with different etiological and pathological characteristics: esophageal squamous cell carcinoma and esophageal adenocarcinoma [2]. In China, esophageal squamous cell carcinoma is the most prevalent histological subtype of esophageal cancer compared to adenocarcinoma in Western countries [3]. If early esophageal cancer can be diagnosed with improved systems, it will substantially decrease both the incidence and mortality [4]. Endoscopy is generally used to detect malignancies in the esophagus; however, inflicted tissue samples are not always visible to the naked eye with an endoscope in early stages of dysplasia, thereby making biopsies random, inefficient, costly, and ultimately unreliable [5, 6]. There is a strong need to develop improved quantitative optical diagnostic techniques for esophageal cancer which is one of the most fatal types of cancer worldwide [7, 8]. Development of improved optical detection methods for functional monitoring and quantification of molecular transport in epithelial tissues as well as the controlling of tissue's optical properties are extremely important for many biomedical applications including therapy, diagnostics, and advanced imaging of devastating diseases such as cancer, arteriosclerosis, diabetic retinopathy, and glaucoma [9]. Since the optical coherence tomography (OCT) was introduced by Huang et al. [10], this technique has been extensively applied in many areas of biomedicine [11–13]. Rapid procedures for tissue diagnosis are important for cancer prevention and therapy. The OCT is a relatively new noninvasive, optical, high-resolution medical and biological imaging technology, which is currently used not only in the research lab but also in clinical practice [14]. At the same time, the OCT is widely employed for cancer detection in various parts of the body including the breast [15], gastrointestinal tract [16], bladder [17], skin [18], oral cavity [19], cervix [20], lung [21], and brain [22]. However, the turbidity of most biological tissues prevents the ability of OCT to be fully engaged in various diagnostic and therapeutic procedures.

Most biological tissues strongly scatter the probe light within the visible and near-IR range. The multiple scattering of light is severely detrimental to imaging contrast and resolution, which limits the effective probing depth for high resolution imaging techniques [23]. There have been several attempts to enhance the imaging depth and reduce the light scattering in tissue for more effective clinical diagnosis. The optical immersion method (optical clearing method) is often used to reduce scattering by applying biocompatible, chemical, optical clearing agents (OCAs) [24–33]. Commonly used OCAs include glycerol, dimethy sulfoxide (DMSO), glucose, trazograph (X-ray contrasting agent), and combinations of such polymers as polypropylene glycol and polyethylene glycol [34–41]. The refractive index of these OCAs ranges from 1.43 to 1.47 [29]. A hyperosmotic agent of glucose was utilised in many studies to increase the depth of light penetration into highly scattering tissues for the imaging technique of near-IR optical coherence tomography [38, 42–48].

Many diseases can alter the physiological structure of the tissue and, thus, affect the permeability rate of molecules into the tissue. Knowing this, the change in the permeability of chemicals and analytes can be used to differentiate abnormal

Qingliang Zhao, Zhouyi Guo, Huajiang Wei MOE Key Laboratory of Laser Life Science & Institute of Laser Life Science, College of Biophotonics, South China Normal University, Guangzhou 510631, China; e-mail: zephanzql@yeah.net, guozhyouyi@yahoo.com.cn, weihj@scnu.edu.cn;
Hongqin Yang, Shusen Xie Key Laboratory of Optoelectronic Science and Technology for Medicine of Ministry of Education of China, Fujian Normal University, Fuzhou 350007, Fujian, China; e-mail: hqyang@fjnu.edu.cn, ssxie@fjnu.edu.cn

Received 25 January 2011; revision received 25 April 2011
Kvantovaya Elektronika **41** (10) 950–955 (2011)
Submitted in English

tissues from healthy ones, which makes it potentially promising for the development of novel early diagnostic methods [49]. The OCT technique has also been recently demonstrated to be a useful tool for monitoring quantifying of the permeability coefficient of different drugs and analytes in various biological tissues (e.g., breast, sclera, cornea, and aorta) *in vitro* or *in vivo* [50–53]. This technique is also suitable for depth-resolved monitoring and quantification of glucose diffusion in sclera with a resolution of ~40 μm [51]. These results suggest that the OCT technique could be successfully applied for functional imaging and quantification of diffusion processes in different types of tissue.

In this paper, we report the results of our pilot studies on the depth-resolved monitoring, differentiation, and quantification of diffusion of the 40% glucose solution in human normal esophagus and esophageal squamous cell carcinoma (ESCC) tissues *ex vivo* by the OCT. We also compare the characteristics of glucose diffusion in these tissues. This method may be useful in detecting, studying, and combating esophageal cancer and may offer the basis of early esophageal cancer diagnosis in the clinical application or medications to achieve the best possible glucose control.

2. Materials and methods

2.1. Materials

After informed consent of the patients undergoing surveillance endoscopy for a diagnosis of ESCC, sixteen fresh specimens from their esophagus were studied by systematic biopsy at the Second Affiliated Clinical Hospital of Guangzhou University of Traditional Chinese Medicine, China. The specimens were divided into two groups: the control group (eight samples) taken from the distant edge of ESCC tissues and the tumour group (eight samples) taken from the centre of ESCC tissues. The methods used to collect and analyse reflectance signals from epithelial tissue have been described previously [54]. The tissues were washed with normal saline solution and sampled immediately after being removed during the operation. Tissue samples were prepared and measurements were taken within 1 h to guarantee minimal changes in the physiological status of the tissues after removal. Before OCT experiments, excess blood was removed by washing with saline solution. The room temperature was maintained at 20 °C throughout the entire experiment. The central baseline in the samples was recorded within 7–10 min before applying the glucose solution. The OCT images were continuously detected for 120 min after application of a hyperosmotic agent – the glucose solution. Topical application of the glucose solution and OCT functional imaging were performed using normal esophagus and ESCC tissues. The 40-wt.% glucose solution was prepared by dissolving 40 g of glucose in 100-ml purified and distilled water. The glucose was purchased from the Tianjin Damao Chemical Reagent Factory, China.

2.2. OCT system

In the experiments, we used a portable time-domain OCT system with a wavelength of 1.310 nm, entirely controlled automatically by a computer. The system provided a bandwidth of about 50 nm and axial resolution of 10–15 μm. The transverse resolution of the system was about 25 μm, determined by the focal spot size produced by the probe beam. The signal-to-noise ratio (SNR) of this system was measured at 100 dB. A 645-nm visible light source was used to adjust the probe beam. Scanning in the reference arm ensured effective change in the sensing/probing depth and point-wise recording of the interference generated an axial scan, known as an (A-scan) consisted of 10000 data points. Lateral scanning (B-scan) was obtained by moving the mirror relative to the tissue sample, which took about 1 s. Two-dimensional images were averaged in the lateral (x axis) (over approximately 1 mm, which was sufficient for speckle noise suppression) direction into a single curve to obtain an OCT signal that represents a one-dimensional in-depth distribution of light. The scheme of the OCT system can be found in [55].

2.3. Methods

The permeability rates of glucose in the human normal esophagus and ESCC tissues were calculated by using optical coherence tomography amplitude (OCTA) method at the different specific depths [56–60]. The OCTA method was used to calculate the permeability rates P_g of 40% glucose solution at each different specific depth in the human normal esophagus and ESCC tissues as:

$$P_g(z) = z/t_z,$$

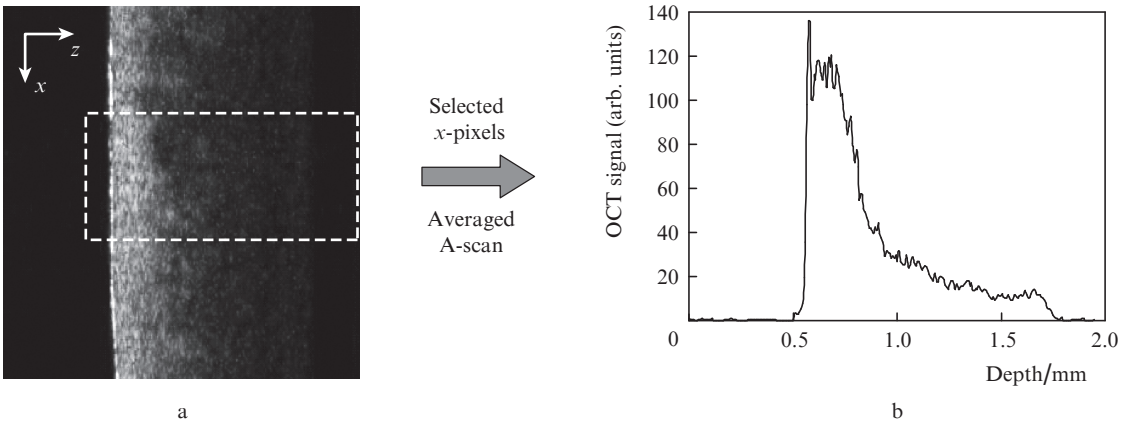

Figure 1. Typical two-dimensional OCT image of human ESCC tissues, 20 min after application of the 40% glucose solution (a) and its corresponding one-dimensional OCT signals (b). The horizontal and vertical axes show the imaging depth and the imaging lateral length, respectively.

where z is the depth at which measurements were performed (calculated from the front surface of tissues) and t_z is the time of glucose diffusion to this depth. The t_z was calculated from the time glucose was added to the tissue until glucose-induced change in the OCT amplitude commenced [10, 51]. The two-dimensional images were averaged in the lateral direction (x axis) into a single curve to obtain an OCT signal that represented a one-dimensional in-depth distribution of light in the logarithmic scale (Fig. 1). The same methods were used to study the analyte diffusion in aorta, corneal and scleral tissues [9, 50, 61, 62], as well as in cancerous tissues [63].

2.4. Statistic analysis

All the data from all samples were presented as a 'mean ± standard deviation' and analysed by a paired-test. All statistical analyses were performed with the statistics software SPSS 10.0 for Windows.

3. Results and discussions

Sixteen esophageal samples have been monitoring using the OCT, taken from the surface at different depths of the tissues. The diffusion process of hyperosmotic agents, monitored for a number of human tissues by the OCT technique, has been reported previously [51, 61, 62]. Figure 2 shows OCT images of the normal esophagus tissues (Figs 2a–d) and ESCC tissues (Figs 2e–h) at 0, 20, 40, and 60 min after application of glucose, respectively. The optical clearing greatly improves OCT imaging of human normal esophageal and ESCC tissues, both in terms of light penetration depth and image quality (Fig. 2). Note, however, that the optical clearing gradually improves with time when glucose diffuses into the intercellular space of normal esophageal and ESCC tissues. This change is explained by the fact that the OCAs applied topically diffuse into the tissues, which results in the matching of the refractive indices between the OCAs and the environment and in efficient reduction of light scattering in the tissue [23, 30].With the diffusion of glucose into internal tissues from the surface of tissues, backscattering decreases by eliminating the refractive index mismatch at tissue–fluid interfaces, and more photons can reach deeper tissue layers. One can see from the comparison of Figs 2a, b, c, d with Figs 2e, f, g, h that scattering in normal esophagus tissues is stronger than that in ESCC tissues. The stronger scattering is likely due to larger nuclei, higher nuclear-to-cytoplasmic ratio in tumour cells and higher regional tumour cell density of the tumour tissues [15]. These results indicate that glucose can significantly enhance the OCT signal not only in normal esophagus tissues but also in ESCC tissues; therefore, the glucose has a potential to become a useful tool for enhancing optical contrast and depth visualisation of optical imaging techniques, including the OCT.

Figure 3a shows the OCT signal as a function of time during glucose diffusion. To quantify the permeability rate of glucose, the monitored specific depths were selected at 56, 105, 175, 315 and 462 μm from tissue surface. One can see that before the diffusion front of the glucose solution reaches the some monitored depth, the OCT signal tends to decrease. At the same time, the OCT signals gradually increase with increasing depth along with the glucose diffusion into the intercellular space. This may be due to the reduction of scattering through refractive index matching within the tissue, caused by the local increase in the glucose concentration [25, 34, 38, 61, 64]. Figure 3b shows the OCT signals change as a function of time recorded at 56, 105, 175, 315 and 462 μm from the ESCC tissues in the process of 40% glucose solution diffusion. We used the same monitoring depth in order to compare the characteristics of glucose permeability in human normal esophageal and ESCC tissues. The human esophagus, as seen from histological sections [65, 66], consists of the following layers (starting from the surface): glandular epithelium, muscularis mucosae, submucosa and muscularis propria. One can see from Fig. 3 the time delay of the glucose front reaching different tissue depths for normal esophagus and ESCC tissues.

The glucose fronts were identified by depth-resolved monitoring of progression of glucose-induced changes in the OCTA with time for the normal esophagus and ESCC tissues. The trends in the OCT signal change at different depths from the ESCC tissues in the case of 40% glucose solution diffusion are similar to those of the normal esophagus tissues. The OCT signal also decreases before the emergence of the glucose front at different monitored depths of the tissue samples, and then gradually increases with glucose diffusion. However, the OCT signal change caused by the glucose solution in the normal

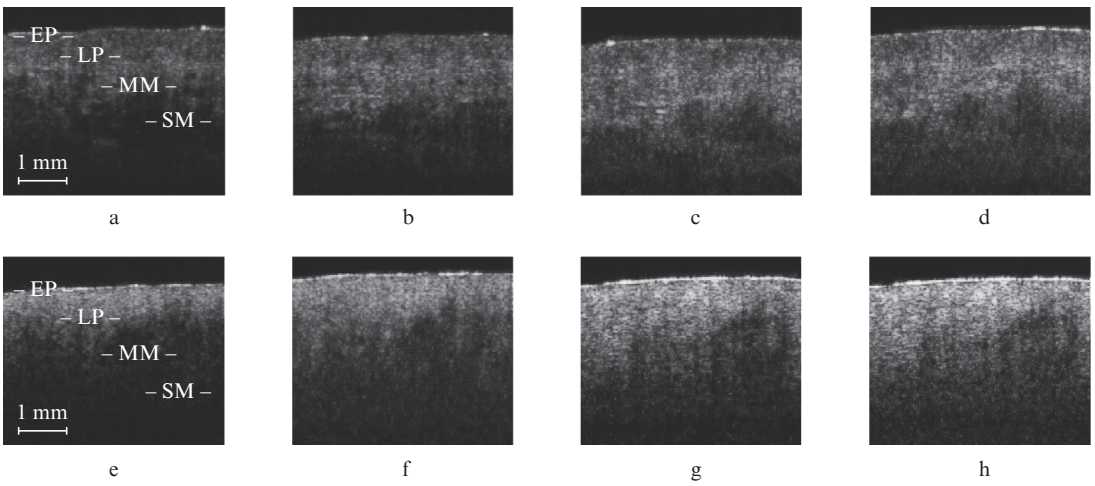

Figure 2. OCT images of the human normal esophagel tissues (a, b, c, d) and the ESCC tissues (e, f, g, h) at 0, 20, 40 and 60 min after application of the 40% glucose solution, respectively: (EP) epithelium; (LP) lamina propria; (MM) muscularis mucosa; (SM) submucosa.

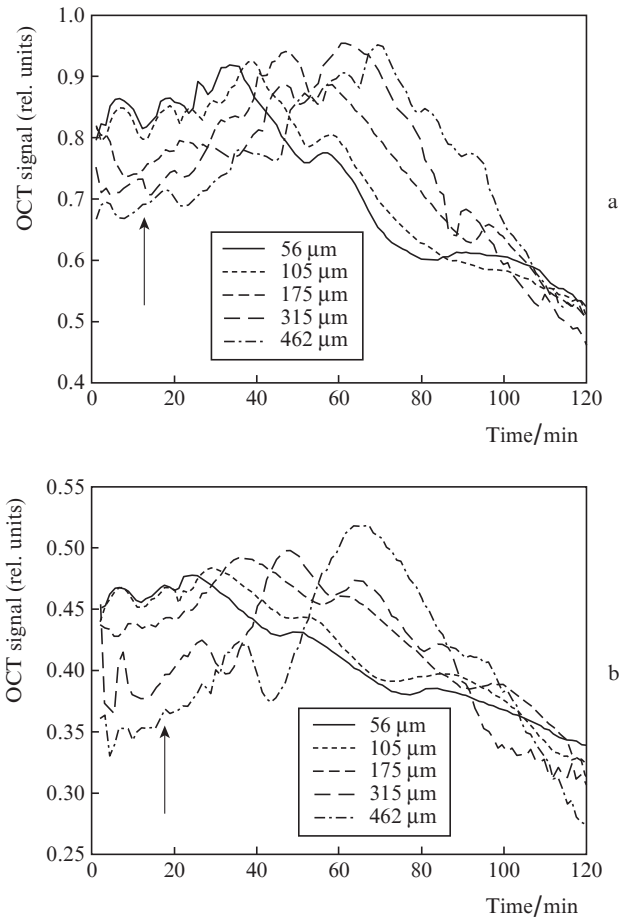

Figure 3. OCT signal as a function of time recorded at different depths during glucose diffusion in the normal esophagus tissues (a) and ESCC tissues (b). The arrows indicate the starting point of glucose diffusion.

esophagus and ESCC tissues are found (see Fig. 3) to be significantly different at the same depth. The OCT signal proves to be higher in the normal esophageal tissues than in the ESCC tissues.

High in-depth resolution of the OCTA technique allows one to calculate glucose permeability rates at different depths of the tissue samples [51]. The permeability rate at each depth is calculated by dividing the thickness of the selected tissue by the time it takes the glucose to diffuse at the monitored depth after the onset of diffusion. Figure 4a presents typical permeability rates P_g of glucose measured at different depths in the normal esophagus tissues by using the OCTA method. One can see that the glucose permeability rate inside the normal esophagus is nonlinear and increases from $(3.30 \pm 0.09) \times 10^{-6}$ cm s^{-1} at the mucous membrane of the normal esophagus tissue to $(1.82 \pm 0.05) \times 10^{-5}$ cm s^{-1} at the submucous layer approximately 742 μm away from the epithelial layer. Figure 4b shows the permeability rates of glucose calculated at different depths of the ESCC tissues. The permeability rate is found to increase from $(1.57 \pm 0.04) \times 10^{-5}$ cm s^{-1} at the mucous membrane of the ESCC tissues to $(3.53 \pm 0.09) \times 10^{-5}$ cm s^{-1} at the submucous layer approximately 742 μm away from the epithelial surface of the ESCC tissues. These results also indicate that the OCT can measure not only the analyte diffusion in specified regions and depths for different types of esophagus tissue but also distinguish normal and malignant human esophagus tissues.

The results of depth-resolved quantification of 40% glucose solution diffusion in Fig. 4 demonstrate that the permeability rates inside normal esophagus and ESCC tissues gradually increase with increasing depth, but in a nonlinear manner. This nonlinearity is due to glucose diffusion through at least two layers: the mucous membrane (low diffusion) and the submucous layer (faster diffusion). The composition of the layers and their thickness can also contribute to the observed curve (Fig. 4), because they may be different at different depths [54]. Comparing Figs 4a and b, we have found that there is a remarkable difference between normal esophageal and ESCC tissues: the permeability rate of 40% glucose solution in the ESCC tissues is higher than that of the normal esophagus tissues at the same depth. However, the permeability rate for the ESCC tissues is lower than that of the normal esophagus tissues. The dissimilarity in the magnitude of the diffusion rate is thought to be a result of the glucose participation in two different diffusion processes at different time intervals in two different tissues of the human esophagus. The experimental results of the depth-resolved monitoring of glucose diffusion and the calculation of the glucose permeability rate in the human normal esophagus and ESCC tissues using OCT technique not only allow us to understand the mechanism of glucose diffusion process but also encourage us to believe that OCTA is an effective method for measuring the permeability rate in specified regions at different esophagus tissue depths. Limitations of the currently utilised OCT system are due to a high

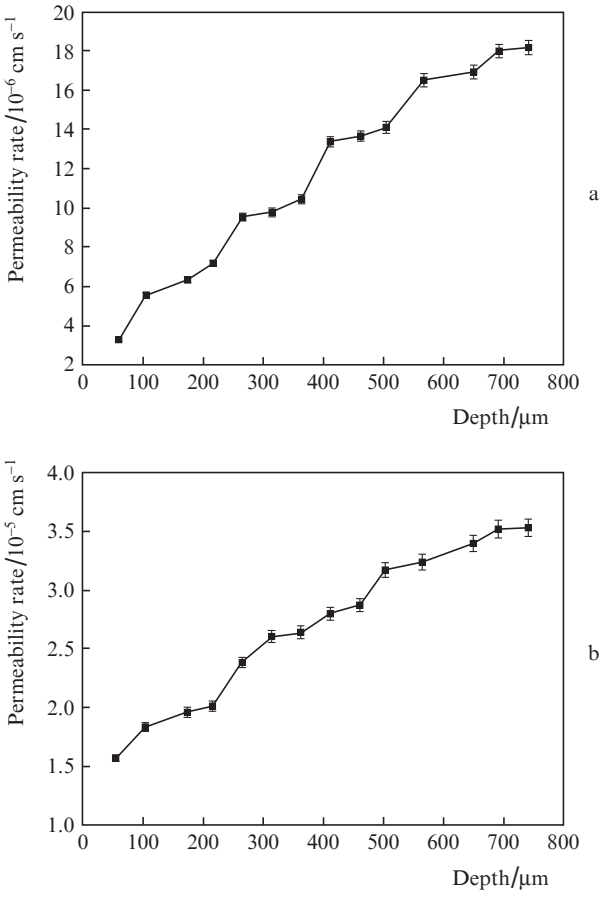

Figure 4. Permeability rates recorded at different depths in the normal esophageal tissue (a) and ESCC tissue (b) during the diffusion of 40% glucose solution. Average standard deviations for the permeability rates are shown over the polyline.

speckle noise and limited resolution. In the future, we will study ultrahigh-resolution OCT systems which make it possible to reduce the observed standard deviation of the glucose permeability rate and choose the optimal concentration of glucose according to different grades of the esophageal cancer using OCT systems.

4. Conclusions

In this paper we have demonstrated the possibility of depth-resolved monitoring, differentiation, and quantifying of glucose diffusion in normal esophagus and ESCC tissues by using the OCT for functional imaging. Using OCT imaging, we have examined the effect of optical clearing, which gradually improves the image quality as the glucose diffuses in the normal esophagus and ESCC tissues. The results obtained indicate the suitability of the OCT for functional imaging of human normal esophagus and ESCC tissues based on depth-resolved quantification of the permeability of biomolecules through these tissues. We have found that the glucose permeability is nonlinear through the tissues and increases with increasing depth in normal esophagus and ESCC tissues, respectively. The results presented can prove the use of OCT in functional imaging and diagnosing of the esophageal tissues as well as in detecting of cancer in esophageal tissues.

Acknowledgements. This work was supported by the National Natural Science Foundation of China (Grant No. 60778047), the Natural Science Foundation of Guangdong Province (Grant No. 06025080), the Key Science and Technology Project of Guangdong Province of China (Grant Nos 2005B50101015 and 2008B090500125), and the Key Science and Technology Project of Guangzhou City of China (Grant No. 2008Z1-D391).

References

1. Edwards B.K., Howe H.L., Ries L.A., Thun M.J., Rosenberg H.M., Yancik R., Wingo P.A., Jemal A., Feigal E.G. *Cancer*, **94**, 2766 (2002).
2. Parkin D.M., Bray F., Ferlay J., Pisani P. *Int. J. Cancer*, **94**, 153 (2001).
3. Du X.L., Hu H., Lin D.C., Xia S.H., Shen X.M., Zhang Y., Luo M.L., Feng Y.B., Cai Y., Xu X., Han Y.L., Zhan Q.M., Wang M.R. *J. Mol. Med.*, **85**, 863 (2007).
4. Wang Q., Yang H., Agrawal A., Wang N.S., Pfefer T.J. *Opt. Express*, **16**, 8685 (2008).
5. Inoue H., Fukami N., Yoshida T. *J. Gastroen. Hepatol.*, **17**, 382 (2002).
6. Tachimori Y.J., Kato H.C. *Critical Reviews in Oncology: Hematology*, **28**, 57 (1998).
7. Parkin D.M., Laara E., Muir C.S. *Int. J. Cancer*, **41**, 184 (1988).
8. Sleisenger M.H., Fordtran J.S. (Eds) *Gastrointestinal Desease: Pathophysiology, Diagnosis, Management* (Philadelphia, W.B.Saunders Co., 1989).
9. Ghosn M.G., Carbajal E.F., Befrui N.A., Tuchin V.V., Larin K.V. *Opt. Lasers Eng.*, **46**, 911 (2008).
10. Ghosn M.G., Tuchin V.V., Larin K.V. *Investigative Ophthalmology & Visual Science*, **48**, 2726 (2007).
11. Huang D., Swanson E.A., Lin C.P., Schuman J.S., Stinson W.G., Chang W., Hee M.R., Flotte T., Gregory K., Puliafito C.A., Fujimoto J.G. *Science*, **254**, 1178 (1991).
12. Fercher A.F., Drexler W., Hitzenberger C.K. *Rep. Prog. Phys.*, **66**, 239 (2003).
13. Podoleanu A.G. *Br. J. Radiol.*, **78**, 976 (2005).
14. Boppart S.A. *Minerva Biotec.*, **16**, 211 (2004).
15. Boppart S.A., Luo W., Marks D.L., Singletary K.W. *Breast Cancer Research and Treatment*, **84**, 85 (2004).
16. Pitris C., Jesser C., Boppart S.A., Stamper D., Brezinski M.E., Fujimoto J.G. *J. Gastroenterology*, **35**, 87 (2000).
17. Zagaynova E., Manyak M.J., Streltsova O., Gladkova N., Feldchtein F., Kamensky V. *J. Clinical Oncology*, **22**, 4538 (2004).
18. Gambichler T., Regeniter P., Bechara F.G., Orlikov A., Vasa R., Moussa G., Stucker M., Altmeyer P., Hoffmann K. *J. Am. Acad. Dermatol.*, **57**, 629 (2007).
19. Wong H.K., Gu S.G., Hammer-Wilson M.J., Epstein J.B., Chen Z.P., Smith P.W. *J. Biomed. Opt.*, **12**, 1 (2007).
20. Escobar P.F., Rojas-Espaillat L., Tisci S., Enerson C., Brainard J., Smith J., Tresser N.J., Feldchtein F.I., Rojas L.B., Belinson J.L. *Int. J. Gynecological Cancer*, **16**, 1815 (2006).
21. Whiteman S.C., Yang Y., Van Pittius D.G., Stephens M., Parmer J., Spiteri M.A. *Clinical Cancer Research*, **12**, 813 (2006).
22. Bohringer H.J., Boller D., Leppert J., Knopp U., Lankenau E., Reusche E., Huttmann G., Giese A. *Lasers Surg. Med.*, **38**, 588 (2006).
23. Wang R.K., Tuchin V.V. *J. X-Ray Sci. Technol.*, **10**, 167 (2002).
24. Tuchin V.V. *J. Phys. D: Appl Phys.*, **38**, 2497 (2005).
25. Tuchin V.V. *IEEE J. Sel. Top. Quantum Electron.*, **13**, 1621 (2007).
26. Galanzha E.I., Tuchin V.V., Solovieva A.V., Stepanova T.V., Luo Q., Cheng H. *J. Phys. D: Appl Phys.*, **36**, 1739 (2003).
27. Tomlins P.H., Wang R.K. *Phys. Med. Biol.*, **47**, 2281 (2002).
28. Wang R.K., Xu X.Q., He Y.H., Elder J.B. *IEEE J. Sel. Top. Quantum Electron.*, **9**, 234 (2003).
29. Choi B., Tsu L., Chen E., Ishak T.S., Iskandar S.M.., Chess S., Nelson J.S. *Lasers Surg. Med.*, **36**, 72 (2005).
30. Stumpp O.F., Welch A.J., Milner T.E., Neev J. *Lasers Surg. Med.*, **37**, 278 (2005).
31. Proskurin S.G., Meglinski I.V. *Laser Phys. Lett.*, **4**, 824 (2009).
32. Larina I.V., Carbajal E.F., Tuchin V.V., Dickinson M.E., Larin K.V. *Laser Phys. Lett.*, **5**, 476 (2008).
33. Petrova G.A., Derpalyuk E., Gladkova N.D., Feldchtein F.I., Nikulin N., Donchenko E., Gelikonov V.M., Kamensky V.A. *Proc. SPIE Int. Soc. Opt. Eng.*, **5140**, 168 (2003).
34. Vargas G., Chan E.K., Barton J.K., Rylander H.G., Welch A.J. *Lasers Surg. Med.*, **24**, 133 (1999).
35. Vargas G., Chan K.F., Thomsen S.L., Welch A.J. *Lasers Surg. Med.*, **29**, 213 (2001).
36. Khan M.H., Chess S., Choi B., Kelly K.M., Nelson J.S. *Lasers Surg. Med.*, **35**, 93 (2004).
37. Khan M.H., Choi B., Chess S., Kelly K.M., McCullough J., Nelson J.S. *Lasers Surg. Med.*, **34**, 83 (2004).
38. Tuchin V.V., Maksimova I.L., Zimnyakov D.A., Kon I.L., Mavlutov A.H., Mishin A. *J. Biomed. Opt.*, **2**, 401 (1997).
39. Xu X., Wang R.K. *Phys. Med. Biol.*, **49**, 457 (2004).
40. Wang R.K., Xu X., Tuchin V.V., Elder J.B. *J. Opt. Soc. Am.*, **18**, 948 (2001).
41. Tuchin V.V. *J. Phys. D: Appl Phys.*, **38**, 2497 (2005).
42. Tuchin V.V. *Tissue Optics: Light Scattering Methods and Instruments for Medical Diagnosis* (Bellingham, WA, SPIE Press, 2000, PM166).
43. Maier J.S., Walker S.A., Fantini S., Franceschini M.A., Gratton E. *Opt. Lett.*, **19**, 2062 (1994).
44. Kohl M., Cope M., Essenpreis M., Bocker D. *Opt. Lett.*, **19**, 2170 (1994).
45. Bruulsema J.T., Hayward J.E., Farrell T.J., Patterson M.S., Heinemann L., Berger M., Koschinsky T., Sandahl-Christiansen J., Orskov H., Essenpreis M., Schmelzeisen-Redeker G., Bücker D. *Opt. Lett.*, **22**, 190 (1997).
46. Tuchin V.V., Zimnyakov D.A., Pravdin A.B. *Proc. SPIE. Int. Soc. Opt. Eng.*, **4001**, 30 (2000).
47. Tuchin V.V. *Proc. SPIE. Int. Soc. Opt. Eng.*, **4162**, 1 (2000).
48. Bashkatov A.N., Genina E.A., Korovina I.V., Kochubey V.I., Sinichkin Y.P., Tuchin V.V. *Proc. SPIE. Int. Soc. Opt. Eng.*, **4224**, 300 (2000).
49. Ghosn M.G., Carbajal E.F., Befrui N., Tellez A., Granada J.F., Larin K.V. *J. Biomed. Opt.*, **13**, 1 (2008).
50. Zhong H.Q., Guo Z.Y., Wei H.J., Zeng C.C., Xiong H.L., He Y.H., Liu S.H. *Laser Phys. Lett.*, **6**, 1 (2009).
51. Ghosn M.G., Tuchin V.V., Larin K.V. *Opt. Lett.*, **31**, 2314 (2006).
52. Larin K.V., Ghosn M.G., Ivers S.N., Tellez A., Granada J.F. *Laser Phys. Lett.*, **4**, 312 (2007).
53. Perelman L.T., Backman V., Wallace M., Zonios G., Manoharan R., Nusrat A., Shields S., Seiler M., Lima C., Hamano T., Itzkan I., VanDam J.J., Crawford J.M., Feld M. *Phys. Rev. Lett.*, **80**, 627 (1998).

54. Larin K.V., Ghosn M.G. *Kvantovaya Elektron*., **36**, 1083 (2006) [*Quantum Electron*., **36**, 1083 (2006)].
55. Dong H.X., Guo Z.Y., Zeng C.C., Zhong H.Q., He Y.H., Wang R.K., Liu S.H. *J. Biomed. Opt.*, **13**, 1 (2008).
56. Larin K.V., Motamedi M., Ashitkov T.V., Esenaliev R.O. *Phys. Med. Biol*., **48**, 1371 (2003).
57. Yeh A.T., Hirshburg J. *J. Biomed. Opt.*, **11**, 1 (2006).
58. Larin K.V., Eledrisi M.S., Motamedi M., Esenaliev R.O. *Diabetes Care*, **25**, 2263 (2002).
59. He Y.H., Wang R.K. *J. Biomed. Opt.*, **9**, 200 (2004).
60. Esenaliev R.O., Larin K.V., Larina I.V., Motamedi M. *Opt. Lett*., **26**, 992 (2001).
61. Larin K.V., Tuchin V.V. *Kvantovaya Elektron*., **38**, 551 (2008) [*Quantum Electronics*., **38**, 551 (2008)].
62. Ghosn M.G., Leba M., Vijayananda A., Rezaee P., Morrisett J.D., Larin K.V. *J. Biophoton.*, **3**, 25 (2009).
63. Xiong H.L., Guo Z., Zeng C., Wang L., He Y., Liu S. *J. Biomed. Opt*., **14**, 1 (2009).
64. Wang R.K., Elder J.B. *Lasers Surg. Med.*, **3**, 201 (2002).
65. Poneros J.M., Brand S., Bouma B.E., Tearney G.J., Compton C.C., Nishioka N.S. *Gastroenterology*, **120**, 7 (2001).
66. Çilesiz I., Fockens P., Kerindongo R., Faber D., Tytgat G., Kate F.T., Leeuwen T.V. *Gastrointestinal Endoscopy*, **56**, 852 (2002).